3D-printed spherical dipole antenna integrated on small RF node

J.J. Adams✉, S.C. Slimmer, J.A. Lewis and J.T. Bernhard

New three-dimensional (3D) printing techniques enable the integration of an antenna directly onto the package of a small wireless sensor node. This volume-filling approach ensures near-optimal bandwidth performance of the small antenna, increasing a system's battery life, data rate or range. Simulated results show that the fabricated spherical antenna's bandwidth-efficiency product is more than half of the fundamental limit and radiation pattern measurements exhibit a dipole pattern with −0.7 dBi gain.

Introduction: The demand for small wireless devices, such as wireless sensor nodes and mobile handsets, continues to grow. Electromagnetic radiation in the ultra-high-frequency (UHF) band, 0.3–3 GHz, has ideal propagation characteristics for non-line-of-sight and mobile communication, but wavelengths in this band are large (10–100 cm) relative to device sizes, making it difficult to generate an efficient broadband radiation mode. As the radiation quality factor (Q) of an antenna increases cubically as the antenna becomes small relative to a wavelength [1, 2], small antennas suffer performance impairments such as narrowband transmission response, difficulty matching to common system impedances and low gain.

A common solution for electrically small packages is to integrate the antenna onto a printed circuit board (PCB) or even a silicon die [3]. Although this is a familiar extension of conventional circuit packaging techniques, it is not the most effective solution for an antenna. As the fundamental limits indicate, the optimal antenna in a small package should circumscribe as much volume as possible. Here, we present a method to design a volumetric antenna on a curved package. The performance of the design closely approaches the performance bounds for any antenna within such a space, and measured radiation patterns using an internal source are presented.

Antenna design: As an electrically small antenna should fill the entire volume for optimal bandwidth performance, the ideal solution for a small sensor node is to print the antenna onto the package itself. To illustrate the relative performance of this approach, consider the design of a communications node in an electrically small, circular-shaped footprint with radius a. If the entire PCB footprint were available for a planar antenna, the minimum possible Q is [2]

$$Q_{\text{min, disc}} \approx \frac{9\pi}{8}\frac{1}{(ka)^3} \tag{1}$$

In contrast, the minimum Q of a sphere of the same radius is [2]

$$Q_{\text{min, sphere}} \approx \frac{3}{2}\frac{1}{(ka)^3} \tag{2}$$

which represents a reduction in Q by a factor of at least 2.36. More likely, only a portion of the PCB is available for the antenna design. Assuming that a circular region of radius $b < a$ is available for the antenna, the reduction in Q is $(3\pi/4)(a/b)^3$, which increases rapidly as the lateral space available for the antenna shrinks.

Integration of the antenna onto a device package often requires a non-planar fabrication method. Recently, additive techniques such as laser direct structuring [4], direct write printing [5, 6] and direct transfer patterning [7] have been used for conformal small antennas. However, none of these results demonstrate a fully encapsulated device that would be suitable for a small sensor node. In this Letter, a fully spherical dipole antenna is printed using direct writing of a silver nanoparticle ink [8] onto the concave (internal) surfaces of two glass hemispheres (thickness = 1.3 mm and diameter = 25.4 mm). A thin circular dielectric substrate (Rogers RT/Duroid 6006, $\varepsilon_r = 6.15$ and height = 1.27 mm) is placed between the two hemispheres and supports batteries and an oscillator. Fig. 1 shows an image of the fabricated antennas. Two 1.5 V batteries (SR66, diameter = 6.8 mm and height = 2.6 mm) are stacked and secured to the PCB with a silver epoxy. On the other side of the PCB, a voltage-controlled oscillator (VCO – SMV1512A, Z-Comm) is soldered onto the board. Vias for the radio-frequency (RF) source and DC bias signals are fed through the board, and the RF and DC signals are separated by several coupling capacitors. The VCO is biased with three VDCs using the batteries, and the control voltage is shorted to give an oscillation frequency of ~1.38 GHz.

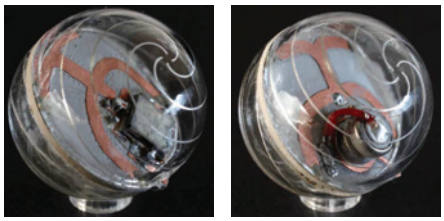

Fig. 1 *Photographs of package-integrated spherical dipole antenna with internal source*

a Top of PCB showing VCO, upper antenna feed and conformal radiating elements
b Bottom of PCB showing battery, lower antenna feed and conformal radiating elements

The design of the radiating element is similar to the four-arm hybrid spherical helix in [6]. Although the hybrid spherical helix is a hemispherical monopole, the ground plane may be removed and replaced with a symmetric reflection of the hemispherical structure to form a dipole. The pitch of the spherical helices is chosen so that they generate a mode that is resonant just below the desired operating frequency. Adjusting the width of the feed lines introduces a distributed capacitance that causes a parallel resonance with adjustable resistance for impedance matching. The cross-shaped planar feed network [5, 6] is modified into a set of curved feed lines as illustrated in Fig. 1 in order to free space on the PCB for the batteries and oscillator. During this process, the feed lines are shaped so that their centrelines are nearly equal in length and vertically symmetric about the plane of the PCB to ensure equal magnitude and phase excitation of the eight helical arms.

Electromagnetic design of the combined board and radiator was performed in the high-frequency structure simulator to generate a matched impedance at the lowest output frequency of the VCO, 1.38 GHz. The simulated return loss of the final antenna design is shown in Fig. 2. The return loss at the centre of the band is 11 dB, and the simulated Q of the antenna calculated from its impedance [9] is 35 at 1.38 GHz. At this electrical size, $ka = 0.367$, the lower bound on Q is 18.1 ([10], eqn. 83) after accounting for the 56.6% simulated radiation efficiency of the antenna. Thus, the antenna's Q is 1.9× greater than the lower bound.

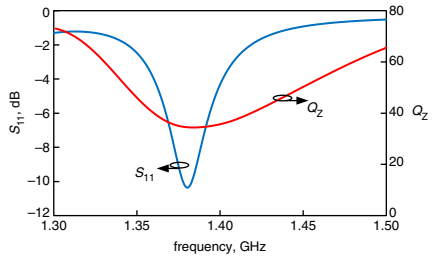

Fig. 2 *Simulated reflection coefficient and Q of spherical dipole*

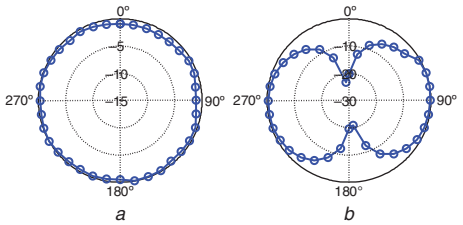

Fig. 3 *Measured co-polar radiation pattern (dB) of spherical dipole at 1.38 GHz*

a *H*-plane cut – plane of PCB
b *E*-plane cut – plane perpendicular to PCB

Measurements: As the RF feed point of this spherical dipole is near the centre of the sphere, it is difficult to directly measure the input impedance of the antenna. However, our previous experience with

hemispherical monopoles [5, 6] has demonstrated that full-wave simulation accurately predicts the measured input impedance of these three-dimensional (3D) antennas (Fig. 2). The radiation properties of the dipole (with internal source) were directly measured in an anechoic chamber at the University of Illinois. The radiated power in the *H*-plane (plane of the PCB) and *E*-plane (plane perpendicular to the PCB) was sampled with a spectrum analyser. The normalised far-field pattern measurements in Fig. 3 show that the antenna operates in a dipole mode, with an omnidirectional pattern in the *H*-plane and a sinusoidal pattern against the elevation angle in the *E*-plane.

To compute the antenna's realised gain, the device output power, free space loss and losses in the receive antenna and cables must be estimated. The output power of the VCO was directly measured while driving a 50 Ω microstrip line. The realised gain of the receive antenna, a dual-polarised conical horn, was measured by placing an identical horn in the chamber and computing the realised gain with cable effects removed via calibration. Losses in the receive cable were found via reflection measurements. Using these data, the peak gain of the package-integrated antenna was measured to be −0.72 dB. Relative to a small dipole's gain of 1.76 dBi, the estimated total antenna efficiency was 57%. This agrees well with simulations showing a total efficiency of 51% and implies the accuracy of the simulated reflection coefficient in Fig. 2.

Conclusion: A fully spherical dipole antenna with an internal source has been fabricated via 3D printing of conductive ink. By distributing the antenna onto the package of a small device rather than in a small PCB footprint, the antenna's bandwidth can more closely approach the fundamental limits. In this case, the antenna's bandwidth-efficiency product is half of the fundamental limit, constrained primarily by the presence of internal conductors and dielectrics.

Acknowledgment: This work was supported under the Intelligence Community Postdoctoral Research Fellowship Program.

17 February 2015
doi: 10.1049/el.2015.0256
One or more of the Figures in this Letter are available in colour online.

J.J. Adams (*Department of Electrical and Computer Engineering, North Carolina State University, Raleigh, NC, USA*)

✉ E-mail: jacob.adams@ncsu.edu

S.C. Slimmer and J.A. Lewis (*School of Engineering and Applied Sciences, Wyss Institute for Biologically Inspired Engineering, Harvard University, Cambridge, MA, USA*)

J.T. Bernhard (*Department of Electrical and Computer Engineering, University of Illinois, Urbana, IL, USA*)

References

1 Chu, L.J.: 'Physical limitations of omni-directional antennas', *J. Appl. Phys.*, 1948, **19**, (12), pp. 1163–1175
2 Yaghjian, A.D., and Stuart, H.R.: 'Lower bounds on the *Q* of electrically small dipole antennas', *IEEE Trans. Antennas Propag.*, 2010, **58**, (10), pp. 3114–3121
3 O, K.K., Kim, K., Floyd, B.A., Mehta, J.L., Yoon, H., Hung, C.-M., Bravo, D., Dickson, T.O., Guo, X., Li, R., Trichy, N., Caserta, J., Bomstad, W.R., Branch, J., Yang, D.-J., Bohorquez, J., Seok, E., Gao, L., Sugavanam, A., Lin, J.-J., Chen, J., and Brewer, J.: 'On-chip antennas in silicon ICs and their application', *IEEE Trans. Electron Devices*, 2005, **52**, (7), pp. 1312–1323
4 Friedrich, A., Geck, B., Klemp, O., and Kellermann, H.: 'On the design of a 3D LTE antenna for automotive applications based on MID technology'. Proc. 2013 European Microwave Conf. (EuMC), Nuremberg, Germany, October 2013, pp. 640–643
5 Adams, J.J., Duoss, E.B., Malkowski, T.F., Motala, M.J., Ahn, B.Y., Nuzzo, R.G., Bernhard, J.T., and Lewis, J.A.: 'Conformal printing of electrically small antennas on three-dimensional surfaces', *Adv. Mater.*, 2011, **23**, (11), pp. 1335–1340
6 Adams, J.J., Slimmer, S.C., Malkowski, T.F., Duoss, E.B., Lewis, J.A., and Bernhard, J.T.: 'Comparison of spherical antennas fabricated via conformal printing: helix, meanderline, and hybrid designs', *IEEE Antennas Wirel. Propag. Lett.*, 2011, **10**, pp. 1425–1428
7 Pfeiffer, C., Xu, X., Forrest, S.R., and Grbic, A.: 'Direct transfer patterning of electrically small antennas onto three-dimensionally contoured substrates', *Adv. Mater.*, 2012, **24**, (9), pp. 1166–1170
8 Ahn, B.Y., Duoss, E.B., Motala, M.J., Guo, X., Park, S.-I., Xiong, Y., Yoon, J., Nuzzo, R.G., Rogers, J.A., and Lewis, J.A.: 'Omnidirectional printing of flexible, stretchable, and spanning silver microelectrodes', *Science*, 2009, **323**, (5921), pp. 1590–1593
9 Yaghjian, A.D., and Best, S.R.: 'Impedance, bandwidth, and *Q* of antennas', *IEEE Trans. Antennas Propag.*, 2005, **53**, (4), pp. 1298–1324
10 Vandenbosch, G.A.E.: 'Reactive energies, impedance, and *Q* factor of radiating structures', *IEEE Trans. Antennas Propag.*, 2010, **58**, (4), pp. 1112–1127